Impact of Grid-forming Converter on Electromechanical Oscillations

Johan Boukhenfouf[1,2]
johan.boukhenfouf@ensam.eu

Xavier Guillaud[1,3]
xavier.guillaud@centralelille.fr

Antoine Bruyere[1,3]
antoine.bruyere@centralelille.fr

[1]Univ. Lille, ULR 2697 - L2EP,F-59000 Lille, France
[2]Arts et Métiers Institute of Technology, F-59000 Lille, France
[3]Centrale Lille, F-59000 Lille, France
[4]Junia, F-59000 Lille, France

This work has been accepted to PowerTech 2023 conference.

***Abstract*—As distributed generation increases, it is essential to study its impact on the grid dynamics. This paper focuses on understanding the influence of the emergent technology of Grid-Forming converters on the electromechanical oscillations of the power system. Interactions among synchronous generators and grid-forming converters are analyzed thanks to simplified models. These highlight the similarities of both sources, and thus, explain the participation of the converter in the oscillation. They also revealed the differences that justify the damping effect of Grid-Forming converter. This conclusion, obtained with simplified models, is validated with a small-signal stability analysis of a detailed model in the dq0-frame.**

***Index Terms*—Power System, Electromechanical Oscillations, Grid-Forming Converters**

I. Introduction

As naturally as a pendulum, the inertia of the synchronous generators (SG) in a power system leads to oscillations among them [1]. However, this analogy must be taken lightly as synchronous machines are much more complicated devices than pendulums. The oscillation depends on various parameters such as grid topology, synchronous generator parameters, control, and operating point, and line loading, among others. So, the instability of such oscillations originates from a coincidence and combination of adverse circumstances as explained in the ENTSO-E incident reports of inter-area oscillations of February 2017 [2] , December 2016 [3], and February 2011 [4].

In the latter, it is concluded that dispersed generation does not influence negatively the power system oscillations. Indeed, per-definition, Grid-following converters track the frequency of the grid, hence they cannot participate in low-frequency modes. However, the penetration of such generation has an indirect impact because it modifies the grid operating point and it replaces synchronous generators. This causes a loss of inertia that lead to an increase of oscillation frequency [5]. However the modification of the operating conditions [6] or the redefinition of the areas [7] challenge this tendency.

Although the previous analysis is true for Grid-Following converters, it is inaccurate for other types of converters, such as Grid-Forming (GFM), also called Virtual Synchronous Machine. Indeed, they are designed to behave like the synchronous generator swing equation, so they inherently participate in the electromechanical modes of the power system. Nevertheless, their impact on the low-frequency oscillations is still unclear in the literature. Only a few studies actually investigate the influence of grid-forming converter on those modes. In these studies, neither a consensus nor a theoretical explanation on the impact of grid-forming converter can be found. While [8] showed that it improves the damping of the electromechanical modes, according to [9] this effect is not observed for inter-area oscillations. In [10], it depends on the quasi-static model that feed the current loop. Finally, [11] claims that an analysis of the participation factors is needed to determine whether the impact will be beneficial or detrimental.

This paper aims to analyze theoretically the electromechanical interactions between GFM and SG thanks to simplified models. This paper aims to analyze theoretically the electromechanical interactions between GFM and SG. A simplified second order model of the synchronous machine is used in this paper. Even if it is well known that this model is not extremely accurate, it is very usefull to have a physical insight of the interaction phenomena. Comparisons with more detailed models of the synchronous machine will be given in order to validate the accuracy of the proposed methodology.

Section II presents the model used for the study. Then, section III investigates the oscillation on a two-generator system in order to understand the impact of Grid-Forming converters. Conclusions drawn are verified on a multi-machine system in section IV. Finally, part V gives the final remarks.

II. Methodology and modeling

A. Small-signal stability analysis

To study electromechanical modes of power system, a small-signal analysis is usually performed. A quick reminder of this method is provided in this part.

The first step is to determine the set of differential-algebraic equations associated with all elements. The sys-

tem can be expressed as (1)-(3) where x is the vector of state variable, z the vector of algebraic variables, u and y respectively correspond to inputs and outputs.

$$\frac{dx}{dt} = f(x, z, u) \tag{1}$$
$$0 = g(x, z, u) \tag{2}$$
$$y = h(x, z, u) \tag{3}$$

Then, these equations are linearized around the operating point to establish the state-space model (4),(5). It is obtained by, first applying the jacobian operator, and then, by isolating Δx and Δy. This methodology is recommended in [12] for small-signal rotor stability studies.

$$\Delta \dot{x} = A\Delta x + B\Delta u \tag{4}$$
$$\Delta y = C\Delta x + D\Delta u \tag{5}$$

$$A = \frac{\partial f}{\partial x} - \frac{\partial f}{\partial z}\left(\frac{\partial g}{\partial z}\right)^{-1}\frac{\partial g}{\partial x} \quad B = \frac{\partial f}{\partial u} - \frac{\partial f}{\partial z}\left(\frac{\partial g}{\partial z}\right)^{-1}\frac{\partial g}{\partial u}$$
$$C = \frac{\partial h}{\partial x} - \frac{\partial h}{\partial z}\left(\frac{\partial g}{\partial z}\right)^{-1}\frac{\partial g}{\partial x} \quad D = \frac{\partial h}{\partial u} - \frac{\partial h}{\partial z}\left(\frac{\partial g}{\partial z}\right)^{-1}\frac{\partial g}{\partial u}$$

Finally, the stability is analyzed through the eigenvalues of the state-matrix A. Each eigenvalue represents a dynamic of the system and it is stable if its real part is negative. Moreover, the more negative the real part is, the faster the dynamic.

The main principles of the small-signal analysis have been presented, chapter 12 of [13] provides more details on the subject.

B. Model of synchronous generator

As a referenced model, the detailed eighth order model of a 900 MW round rotor synchronous machine is used. It is equipped with transformer, static excitation system ST1C, PSS1A [14], and governor IEESGO [15] as showed in Fig.1. Equations, models and parameters for these systems are available in [16] or [13]. However, in this work, the nominal frequency is 50 Hz.

As the nature of SG and converters are quite different, analyzing the interactions between them is not straight forward. This is why, simplified models of are employed in this work. For generators, the classical model is employed as in [17]. It is a constant voltage source behind impedance (Fig.2) whose angle is driven by the swing equation (Fig.3).

This model is interesting because it highlights the second order dynamics of the generator and thus it enables simple theoretical analysis. Moreover, with the right set of parameters, the results obtained for low-frequency dynamics are satisfactory as showed by [18] where parameters are estimated from phasor measurements.

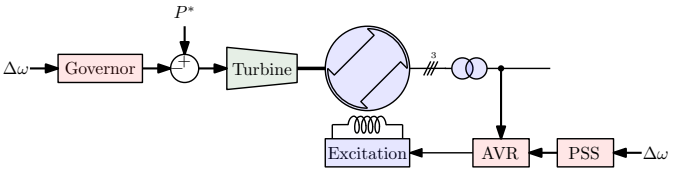

Fig. 1. Detailed model of synchronous generator

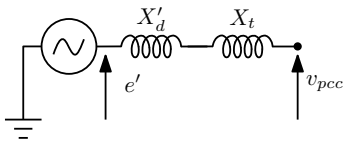

Fig. 2. Quasi-static model of synchronous generator

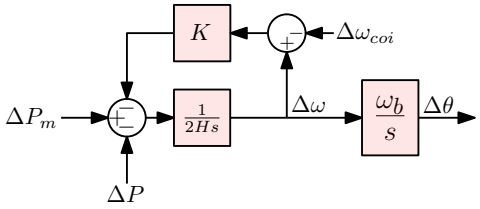

Fig. 3. Simplified model of synchronous generator

C. Model of grid-forming converter

The referenced model of the converter is depicted in Fig.4. For the equations, the VSC with constant DC bus is represented by an average model. The power control is realized through the angle as represented in Fig.6. Reference voltage amplitudes v_d^*, v_q^* are respectively 1, 0 and are adapted by the transient virtual resistance [19]. The parameters of the converter are given in table I.

The classical model of the generator is established under strong hypothesis that includes the quasi-static model of the grid and the disregard of fast dynamics. By applying these to the grid-forming, the same type of simplified model can be determined : a constant voltage source behind an impedance (Fig.2) whose angle is driven by the power control (Fig.3).

Note that the hypotheses used to established the simplified model of the converter is but an extract of all approximations necessary for the generator classical model. Indeed, all controllers and the machine are aggregated into the second order representation, whereas, for the converter, only fast dynamics, such as internal control and electromagnetic flux variations, are neglected. Moreover, the damping coefficient is a control parameter, so it is known. Hence, the accuracy of the simplified model of converter is better than that of the generator.

D. Model of the grid

The reference model of the grid correspond to Kirchhof's laws in the dq-frame. The simplified model need to comply with the input/output of the sources which are the power and the angle. Therefore, the convenient representation of

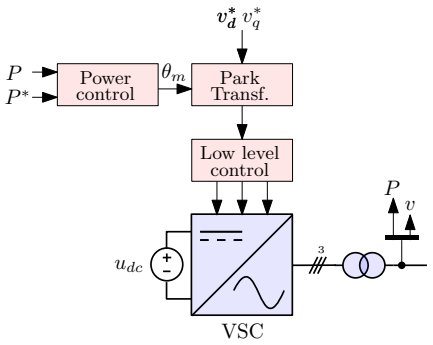

Fig. 4. Detailed model of grid-forming converter

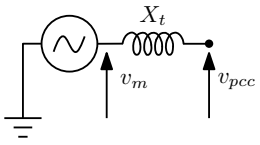

Fig. 5. Quasi-static model of grid-forming converter

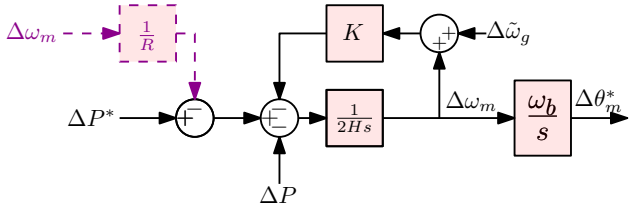

Fig. 6. Power control of grid-forming converter

TABLE I
GFM Parameters

Parameter	Value	
Nominal frequency (f_n)	50	Hz
Nominal power (P_n)	900	MW
Connection voltage (U_n)	230	kV
Converter voltage (U_{vsc})	20	kV
Transformer resistance (R_t)	0.005	p.u
Transformer reactance (X_t)	0.15	p.u
Inertia (H)	5	s
Damping coefficient (K)	333	p.u
Transient virtual resistance (R_v)	0.09	p.u
Transient virtual resistance bandwidth (ω_v)	60	rad/s
PLL integral constant (K_i)	0.61	
PLL proportional constant (K_p)	29.34	

the grid corresponds to the synchronizing torque matrix. A brief summary on its calculation is provided in this section, for detailed explanation, please refer to appendix D of [16] or chapter two of [20].

In the grid, where a power sources is connected, the power ($\Delta P_d = [\Delta P_1 \dots \Delta P_k]^T$) depends on the angle ($\Delta\delta_d = [\Delta\delta_1 \dots \Delta\delta_k]^T$). On other nodes, the power is independent ($\Delta P_i = [\Delta P_m \dots \Delta P_n]^T$). For the connection of the simplified models, ΔP_d should be expressed as a linear function of $\Delta\delta_d$ and ΔP_i as in (6).

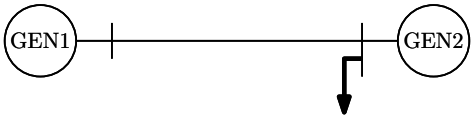

Fig. 7. Two-generator test bed

$$\Delta P_d = K_s \Delta\delta_d + K_{ps} \Delta P_i = \begin{bmatrix} K_s & K_{ps} \end{bmatrix} \begin{bmatrix} \Delta\delta_d \\ \Delta P_i \end{bmatrix} \tag{6}$$

K_s (7) and K_{ps} (8) are retrieved from the derivation of power expressions (9) for both dependent and independent power nodes. The hypothesis to have these expressions is the standard P-δ, Q-V decoupling.

$$K_s = \frac{\partial P_d}{\partial \delta_i} - \frac{\partial P_d}{\partial \delta_d} \left(\frac{\partial P_i}{\partial \delta_d} \right)^{-1} \frac{\partial P_i}{\partial \delta_i} \tag{7}$$

$$K_{ps} = \frac{\partial P_d}{\partial \delta_d} \left(\frac{\partial P_i}{\partial \delta_d} \right)^{-1} I \tag{8}$$

$$P_i = V_i \sum_{k=1}^{n} V_k Y_{ik} cos(\theta_{ik} + \delta_k - \delta_i) \tag{9}$$

V_i, δ_i are the voltage magnitude and phase of node i and Y_{ik}, θ_{ik} are the magnitude and phase of the admittance between node i and node k.

As an example, consider the converter of Fig.2 connected to a thevenin equivalent with an impedance X_{th}. The power transmitted can be expressed as in (10) and the corresponding synchronizing torque is given in (11). Remark that the impedance of the power source is included in the coupling matrix.

$$P = \frac{V_m V_{pcc}}{X_t + X_{th}} sin(\delta_m - \delta_p cc) \tag{10}$$

$$K_s = \frac{dP}{d\delta_m} = \frac{V_{m0} V_{pcc0}}{X_t + X_{th}} cos(\delta_{m0} - \delta_{pcc0}) \tag{11}$$

The present section have reminded the methodology of the small-signal stability analysis that is used in this work. Both reference and simplified model of the elements have been explained. Next section will analyze the impact of grid-forming converter on the electromechanical oscillation of a simple grid.

III. Study of the two-generator system

To investigate the electromechanical interactions between GFM and SG, the simple two-generator test-bed of Fig.7 is used. The generators presented in section II are connected with a line of 125 km and a load is added at the connection point of GEN2. It is reminded that generators are considered with their transformer. Parameters of the line and operating point are given respectively in table II and III.

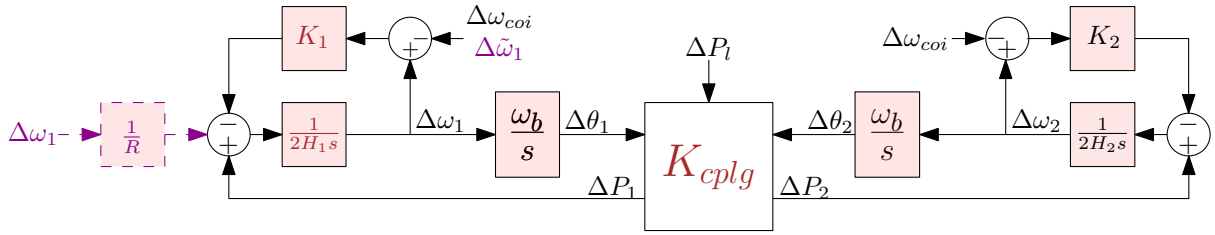

Fig. 8. Simplified model of the two-generator test-bed. (In black, synchronous machines parameters in both cases. In brown, parameter values changed when GEN1 is replaced. In magenta, input changed when GEN1 is replaced.)

TABLE II
LINE PARAMETERS

Parameter	Value	
Nominal frequency (f_n)	50	Hz
Base power (P_n)	100	MW
Nominal Voltage (U_n)	230	kV
Resistance(r_d)	0.0001	p.u/fm
Inductance (x_d)	0.001	p.u/km
Susceptance (b_d)	0.00175	p.u/km

TABLE III
OPERATING POINT ($S_{base} = 100$ MW, $U_{base} = 230$ KV)

Device	Type	P (p.u)	Q (p.u)	V (p.u)	δ (°)
LOAD	PQ	12.6	0.5	1	0
GEN1	PV	6.32	246.7	1	54.0
GEN2	Swing	6.88	444.16	1	0

A. Base case: two synchronous generators

First, as a reference and validation scenario, GEN1 and GEN2 are synchronous machines with the same parameters as in section II. Fig.8 presents (in black line) the simplified model of the whole system. The damping coefficients have been estimated by trial and error and fixed to $K_1 = K_2 = 8$ to match the response of the reference detailed model. The coupling matrix is given in (12).

$$K_{cplg} = \begin{bmatrix} 3.965 & -3.965 & -0.166 \\ -3.134 & 3.134 & -0.869 \end{bmatrix}_{S_b=100\text{MVA}} \tag{12}$$

The representation of Fig.8 is interesting to understand the oscillation between the machines. The inertias swing against each other through the grid. Furthermore, it is possible to identify analytically the oscillation according to the load step applied. This theoretical expression is given in (13).

$$\frac{\Delta\omega_{12}}{\Delta P_l} = \frac{\frac{H_1K_{23}-H_2K_{13}}{2H_1H_2}}{s^2 + \frac{H_1K_2+H_2K_1}{4H_1H_2}s + \frac{\omega_b(H_1K_{22}+H_2K_{11})}{2H_1H_2}} \tag{13}$$

$$\begin{cases} \omega_n = \sqrt{\frac{\omega_b(H_1K_{22}+H_2K_{11})}{2H_1H_2}} \\ \xi = \frac{H_1K_2+H_2K_1}{4\sqrt{2\omega_b H_1H_2(H_1K_{22}+H_2K_{11})}} \end{cases} \tag{14}$$

TABLE IV
EIGENVALUES OF THE OSCILLATION MODE OF THE TWO-GENERATOR TEST BED WITH TWO SGS

Model	Eigenvalues	Natural Frequency	Damping
Detailed	$-0.27352 \pm j4.3322$	0.69086	0.063012
Simplified	$-0.33892 \pm j4.5486$	0.72595	0.074305

For the case study, the simplified model gives satisfactory results for the dominant poles of the system including the electromechanical oscillation. It is confirmed by the results of the small-signal stability analysis for both detailed and simplified models that are displayed in Table IV.

B. Replacement with a grid-forming converter

To analyze the impact of GFM on the oscillation, GEN1 is replaced with a GFM. Parameters are the same as in table I. The synchronous machine damping coefficient, which needs to be evaluated case by case, has been kept at 8 because the operating conditions have barely changed between both scenarios.

Results displayed in Fig.9 show a loss in the accuracy of the simplified model. It probably comes from the previous choice not to adapt the damping coefficient of the machine. Moreover, the solution provided by the simplified model is still satisfactory. Indeed, the impact of the grid-forming is the same for both models: a higher natural frequency and a better damping. Thanks to the simplified model established in section II, a comparison between GFM and SG is simple and helpful to understand this observation.

First, highlighted by Fig.2 and 5, the impedance of connection is smaller for GFM. Indeed, the latter only has the inductance of the transformer while the machine adds its internal transient inductance. This decrease of electrical distance induces a higher synchronizing torque (15) that lead to a higher natural frequency as proved by (14).

$$K_{cplg} = \begin{bmatrix} 4.509 & -4.509 & -0.189 \\ -3.540 & 3.540 & -0.852 \end{bmatrix}_{S_b=100\text{MVA}} \tag{15}$$

The second distinction is the parameters of the systems. For GFMs, they are control parameters and can be tuned to response as wanted. The inertia is fixed to comply

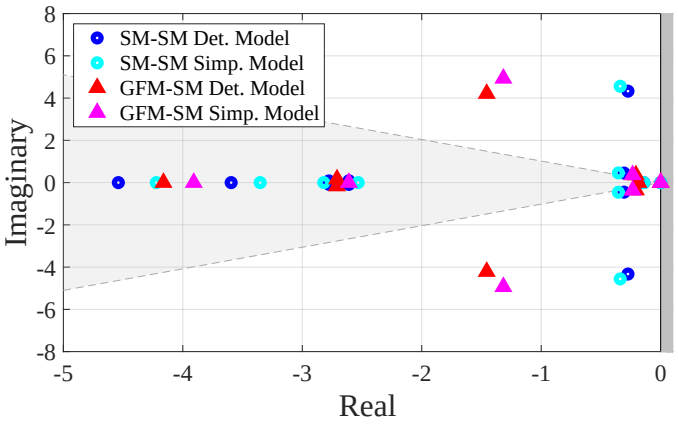

Fig. 9. Pole maps of the two-generator system

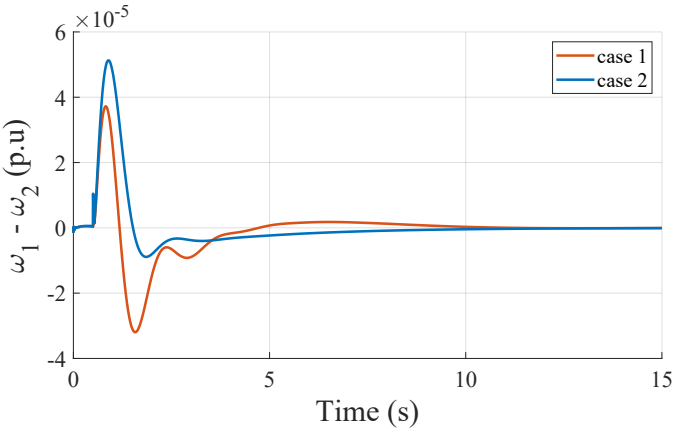

Fig. 10. Frequency oscillation between the generator

TABLE V
DROOP DISTRIBUTION BETWEEN THE GENERATORS

	Droop coef. (R)	
Case	GEN1	GEN2
1	-	2%
2	4%	4%

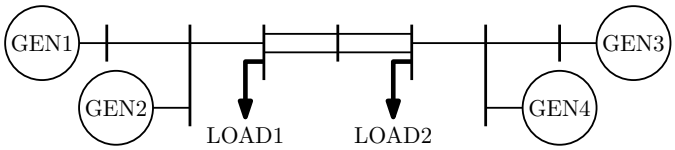

Fig. 11. Two-area four-generator system

with system needs, it is often chosen similar as the one of synchronous machines ($H \approx 5/6$ s). The damping, on the other end, can be chosen much higher than the natural physical damping of SGs. Hence, power system oscillations are better damped with GFMs than with SGs.

C. Impact of droop control in the GFm

There is one more difference between SM and GFM that can modify power system oscillation when a substitution is done. The fast power response of converter compared to mechanical power response of a turbine. So, when a droop is applied with a converter, another loop of damping is created as showed in magenta in Fig.8. For a synchronous machine, that loop does exist but it is too slow to affect significantly the oscillation.

To illustrate the impact of the droop, a case with and without droop control by the converter were simulated. Table V display the droop parameter of the generators and Fig.10 show the oscillating behavior of the detailed model. As expected, the droop control by a grid-forming converter adds a supplementary damping effect.

IV. STUDY OF A MULTI-MACHINE SYSTEM

In order to confirm the conclusions drawn in the previous section, a mutli-machine system is analyzed in this section. It is the traditional Klein-Rogers-Kundur system exhibited in Fig.11. Its parameter are available in chapter 12 of [13]. The operating point used is presented in table VI.

First, all generators are synchronous machines. Then GEN1 is replaced with a GFM, so area one becomes a mixed area. Finally, GEN2 is replaced and area one is a full power electronic area. Small-signal stability analysis

TABLE VI
OPERATING POINT OF THE TWO-AREAS SYSTEM ($S_{base} = 100$ MVA, $U_{base} = 230$ KV)

Device	Type	P (p.u)	Q (p.u)	V (p.u)	δ (°)
LOAD1	PQ	9.67	0.5	0.98	-1.65
LOAD2	PQ	13.67	1	0.97	-24.0
GEN1	PV	6	-0.23	1	13.9
GEN2	PV	6	2.96	1	8.24
GEN3	swing	6.02	0.35	1	0
GEN4	PV	6	3.76	1	-8.4345

is carried out for each case. The results are presented in Fig.12.

On one hand, as SGs are replaced by GFMs, both natural frequency and damping of the local mode of area one increase. This phenomenon is expected according to the study of the previous section. On the other hand, the intra-area mode of area two is left completely unchanged. It seems reasonable because generators in area one do not participate in this mode whether they are SGs or GFMs.

Ultimately, the inter-area mode also behave as explained with the two-generator model. Its natural frequency increases and its damping increases. This can be explained if areas are considered as one aggregated generator. With this representation, the system is similar as the two-generator test bed, hence conclusions from the latter also apply to the inter-area mode.

It is remarked that the increase of natural frequency of the inter-area oscillations is less pronounced than the one of the intra-area mode. Indeed, as the line length enlarges, the influence of the withdrawal of SGs internal impedance decreases.

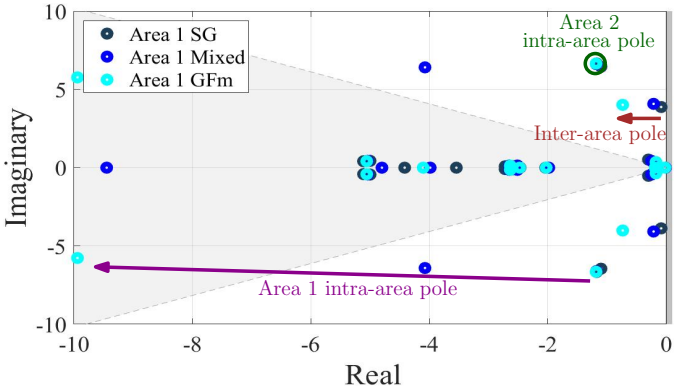

Fig. 12. Impact of replacing SGs with GFMs in area 1 of the two-area four-generator system

V. Conclusion

In this paper, simplified models of the synchronous machine and the grid forming converter have been used. Combined with a simplified model of the grid, it is possible to develop some block diagrams which show clearly the electromechanical interaction between the synchronous machine and the grid forming converter. From this model, it is possible to derive some key conclusions:

1) The substitution from a synchronous machine to a grid forming converter is always damping the system.
2) It is possible to derive some analytical formula which gives a good approximation of the electromechanical interaction between a synchronous machine and a grid forming converter.
3) Due to the highest speed of the grid forming converter, the frequency droop control is providing a significant damping to the system to which the converter is connected.

The methodology presented requires to be tested on others power system in order to totally validate the findings. The results should also be checked if the DC bus is replaced by a more realistic primary source. Finally, to go further, the models presented here can be exploited for the determination of aggregated model of power systems.

References

[1] G. Rogers, *Power system oscillations*, 2000, oCLC: 851737563. [Online]. Available: http://public.ebookcentral.proquest.com/choice/publicfullrecord.aspx?p=3080721

[2] "Oscillation Event 03.12.2017," ENTSO-E, Tech. Rep., Mar. 2018. [Online]. Available: https://eepublicdownloads.entsoe.eu/clean-documents/SOC%20documents/Regional_Groups_Continental_Europe/OSCILLATION_REPORT_SPD.pdf

[3] "Analysis of CE inter-area oscillation of 1st December 2016," ENTSO-E, Tech. Rep., Jul. 2017. [Online]. Available: https://eepublicdownloads.entsoe.eu/clean-documents/SOC%20documents/Regional_Groups_Continental_Europe/2017/CE_inter-area_oscillations_Dec_1st_2016_PUBLIC_V7.pdf

[4] "Analysis of CE inter-area oscillations of 19 and 24 february 2011," ENTSO-E, Tech. Rep., Aug. 2011. [Online]. Available: https://eepublicdownloads.entsoe.eu/clean-documents/pre2015/publications/entsoe/RG_SOC_CE/Top7_110913_CE_inter-area-oscil_feb_19th_24th_final.pdf

[5] R. Elliott, R. Byrne, A. Ellis, and L. Grant, "Impact of increased photovoltaic generation on inter-area oscillations in the Western North American power system," in *2014 IEEE PES General Meeting | Conference Exposition*, Jul. 2014, pp. 1–5, iSSN: 1932-5517.

[6] H. H. Askari, S. Hashemi, R. Eriksson, and Q. Wu, "Effect of full converter wind turbines on inter-area oscillation of power systems," in *2015 International Conference on Clean Electrical Power (ICCEP)*, Jun. 2015, pp. 270–276.

[7] H. R. Chamorro, M. Ghandhari, and R. Eriksson, "Influence of the increasing non-synchronous generation on Small Signal Stability," in *2014 IEEE PES General Meeting | Conference Exposition*, Jul. 2014, pp. 1–5, iSSN: 1932-5517.

[8] M. Baruwa and M. Fazeli, "Impact of Virtual Synchronous Machines on Low-Frequency Oscillations in Power Systems," *IEEE Transactions on Power Systems*, vol. 36, no. 3, pp. 1934–1946, May 2021, conference Name: IEEE Transactions on Power Systems.

[9] X. Zhou, S. Cheng, X. Wu, and X. Rao, "Influence of Photovoltaic Power Plants based on VSG Technology on Low Frequency Oscillation of Multi-machine Power Systems," *IEEE Transactions on Power Delivery*, pp. 1–1, 2022, conference Name: IEEE Transactions on Power Delivery.

[10] D. Sun, Y. Li, Q. Wang, Y. Luo, H. Liu, and F. Zhao, "Impact of Virtual Synchronous Generators on Inter-Area Low Frequency Oscillation," in *2020 5th Asia Conference on Power and Electrical Engineering (ACPEE)*, Jun. 2020, pp. 498–502.

[11] M. Chen, D. Zhou, and F. Blaabjerg, "High penetration of inverter-based power sources with VSG control impact on electromechanical oscillation of power system," *International Journal of Electrical Power & Energy Systems*, vol. 142, p. 108370, Nov. 2022. [Online]. Available: https://linkinghub.elsevier.com/retrieve/pii/S0142061522003854

[12] "IEEE Guide for Synchronous Generator Modeling Practices and Parameter Verification with Applications in Power System Stability Analyses," *IEEE Std 1110-2019 (Revision of IEEE Std 1110-2002)*, pp. 1–92, Mar. 2020, conference Name: IEEE Std 1110-2019 (Revision of IEEE Std 1110-2002).

[13] P. Kundur, *Power System Stability and Control*, 1st ed. McGraw - Hill, 1994.

[14] "IEEE Recommended Practice for Excitation System Models for Power System Stability Studies," *IEEE Std 421.5-2016 (Revision of IEEE Std 421.5-2005)*, pp. 1–207, Aug. 2016, conference Name: IEEE Std 421.5-2016 (Revision of IEEE Std 421.5-2005).

[15] "Dynamic Models for Turbine-Governors in Power System Studies," IEEE Power & Energy Society, Tech. Rep., Jan. 2013. [Online]. Available: https://site.ieee.org/fw-pes/files/2013/01/PES_TR1.pdf

[16] G. Santos Pereira, "Stability of power systems with high penetration of sources interfaced by power electronics," PhD Thesis, 2020. [Online]. Available: http://www.theses.fr/2020CLIL0018/document

[17] L. Benedetti, P. N. Papadopoulos, and A. Egea-Alvarez, "Small Signal Interactions Involving a Synchronous Machine and a Grid Forming Converter," in *2021 IEEE Madrid PowerTech*. Madrid, Spain: IEEE, Jun. 2021, pp. 1–6. [Online]. Available: https://ieeexplore.ieee.org/document/9494923/

[18] M. Shiroei, B. Mohammadi-Ivatloo, and M. Parniani, "Low-order dynamic equivalent estimation of power systems using data of phasor measurement units," *International Journal of Electrical Power & Energy Systems*, vol. 74, pp. 134–141, 2016. [Online]. Available: https://www.sciencedirect.com/science/article/pii/S0142061515003014

[19] T. Qoria, "Grid-forming control to achieve a 100% power electronics interfaced power transmission systems," phdthesis, HESAM Université, Nov. 2020. [Online]. Available: https://pastel.archives-ouvertes.fr/tel-03078479

[20] J. H. Chow, Ed., *Power System Coherency and Model Reduction*, ser. Power Electronics and Power Systems. New York, NY: Springer New York, 2013, vol. 94. [Online]. Available: http://link.springer.com/10.1007/978-1-4614-1803-0